

Measurement of absolute branching fraction of the inclusive decay $\Lambda_c^+ \rightarrow \Lambda + X$

M. Ablikim¹, M. N. Achasov^{9,d}, S. Ahmed¹⁴, M. Albrecht⁴, M. Alekseev^{53A,53C}, A. Amoroso^{53A,53C}, F. F. An¹, Q. An^{50,40}, J. Z. Bai¹, Y. Bai³⁹, O. Bakina²⁴, R. Baldini Ferroli^{20A}, Y. Ban³², D. W. Bennett¹⁹, J. V. Bennett⁵, N. Berger²³, M. Bertani^{20A}, D. Bettoni^{21A}, J. M. Bian⁴⁷, F. Bianchi^{53A,53C}, E. Boger^{24,b}, I. Boyko²⁴, R. A. Briere⁵, H. Cai⁵⁵, X. Cai^{1,40}, O. Cakir^{43A}, A. Calcaterra^{20A}, G. F. Cao^{1,44}, S. A. Cetin^{43B}, J. Chai^{53C}, J. F. Chang^{1,40}, G. Chelkov^{24,b,c}, G. Chen¹, H. S. Chen^{1,44}, J. C. Chen¹, M. L. Chen^{1,40}, P. L. Chen⁵¹, S. J. Chen³⁰, X. R. Chen²⁷, Y. B. Chen^{1,40}, X. K. Chu³², G. Cibinetto^{21A}, H. L. Dai^{1,40}, J. P. Dai^{35,h}, A. Dbeyssi¹⁴, D. Dedovich²⁴, Z. Y. Deng¹, A. Denig²³, I. Denysenko²⁴, M. Destefanis^{53A,53C}, F. De Mori^{53A,53C}, Y. Ding²⁸, C. Dong³¹, J. Dong^{1,40}, L. Y. Dong^{1,44}, M. Y. Dong^{1,40,44}, Z. L. Dou³⁰, S. X. Du⁵⁷, P. F. Duan¹, J. Fang^{1,40}, S. S. Fang^{1,44}, X. Fang^{50,40}, Y. Fang¹, R. Farinelli^{21A,21B}, L. Fava^{53B,53C}, S. Fegan²³, F. Feldbauer²³, G. Felici^{20A}, C. Q. Feng^{50,40}, E. Fioravanti^{21A}, M. Fritsch^{23,14}, C. D. Fu¹, Q. Gao¹, X. L. Gao^{50,40}, Y. Gao⁴², Y. G. Gao⁶, Z. Gao^{50,40}, B. Garillon²³, I. Garzia^{21A}, K. Goetzen¹⁰, L. Gong³¹, W. X. Gong^{1,40}, W. Gradl²³, M. Greco^{53A,53C}, M. H. Gu^{1,40}, S. Gu¹⁵, Y. T. Gu¹², A. Q. Guo¹, L. B. Guo²⁹, R. P. Guo^{1,44}, Y. P. Guo²³, Z. Haddadi²⁶, S. Han⁵⁵, X. Q. Hao¹⁵, F. A. Harris⁴⁵, K. L. He^{1,44}, X. Q. He⁴⁹, F. H. Heinsius⁴, T. Held⁴, Y. K. Heng^{1,40,44}, T. Holtmann⁴, Z. L. Hou¹, C. Hu²⁹, M. H. Hu^{1,44}, T. Hu^{1,40,44}, Y. Hu¹, G. S. Huang^{50,40}, J. S. Huang¹⁵, X. T. Huang³⁴, X. Z. Huang³⁰, Z. L. Huang²⁸, T. Hussain⁵², W. Ikegami Andersson⁵⁴, Q. Ji¹, Q. P. Ji¹⁵, X. B. Ji^{1,44}, X. L. Ji^{1,40}, X. S. Jiang^{1,40,44}, X. Y. Jiang³¹, J. B. Jiao³⁴, Z. Jiao¹⁷, D. P. Jin^{1,40,44}, S. Jin^{1,44}, Y. Jin⁴⁶, T. Johansson⁵⁴, A. Julin⁴⁷, N. Kalantar-Nayestanaki²⁶, X. L. Kang¹, X. S. Kang³¹, M. Kavatsyuk²⁶, B. C. Ke⁵, T. Khan^{50,40}, A. Khoukaz⁴⁸, P. Kiese²³, R. Kliemt¹⁰, L. Koch²⁵, O. B. Kolcu^{43B,f}, B. Kopf⁴, M. Kornicer⁴⁵, M. Kuemmel⁴, M. Kuessner⁴, M. Kuhlmann⁴, A. Kupsc⁵⁴, W. Kühn²⁵, J. S. Lange²⁵, M. Lara¹⁹, P. Larin¹⁴, L. Lavezzi^{53C}, S. Leiber⁴, H. Leithoff²³, C. Leng^{53C}, C. Li⁵⁴, Cheng Li^{50,40}, D. M. Li⁵⁷, F. Li^{1,40}, F. Y. Li³², G. Li¹, H. B. Li^{1,44}, H. J. Li^{1,44}, J. C. Li¹, K. J. Li⁴¹, Kang Li¹³, Ke Li³⁴, Lei Li³, P. L. Li^{50,40}, P. R. Li^{44,7}, Q. Y. Li³⁴, T. Li³⁴, W. D. Li^{1,44}, W. G. Li¹, X. L. Li³⁴, X. N. Li^{1,40}, X. Q. Li³¹, Z. B. Li⁴¹, H. Liang^{50,40}, Y. F. Liang³⁷, Y. T. Liang²⁵, G. R. Liao¹¹, D. X. Lin¹⁴, B. Liu^{35,h}, B. J. Liu¹, C. X. Liu¹, D. Liu^{50,40}, F. H. Liu³⁶, Fang Liu¹, Feng Liu⁶, H. B. Liu¹², H. M. Liu^{1,44}, Huanhuan Liu¹, Huihui Liu¹⁶, J. B. Liu^{50,40}, J. Y. Liu^{1,44}, K. Liu⁴², K. Y. Liu²⁸, Ke Liu⁶, L. D. Liu³², P. L. Liu^{1,40}, Q. Liu⁴⁴, S. B. Liu^{50,40}, X. Liu²⁷, Y. B. Liu³¹, Z. A. Liu^{1,40,44}, Zhiqing Liu²³, Y. F. Long³², X. C. Lou^{1,40,44}, H. J. Lu¹⁷, J. G. Lu^{1,40}, Y. Lu¹, Y. P. Lu^{1,40}, C. L. Luo²⁹, M. X. Luo⁵⁶, X. L. Luo^{1,40}, X. R. Lyu⁴⁴, F. C. Ma²⁸, H. L. Ma¹, L. L. Ma³⁴, M. M. Ma^{1,44}, Q. M. Ma¹, T. Ma¹, X. N. Ma³¹, X. Y. Ma^{1,40}, Y. M. Ma³⁴, F. E. Maas¹⁴, M. Maggiora^{53A,53C}, Q. A. Malik⁵², Y. J. Mao³², Z. P. Mao¹, S. Marcello^{53A,53C}, Z. X. Meng⁴⁶, J. G. Messchendorp²⁶, G. Mezzadri^{21B}, J. Min^{1,40}, T. J. Min¹, R. E. Mitchell¹⁹, X. H. Mo^{1,40,44}, Y. J. Mo⁶, C. Morales Morales¹⁴, G. Morello^{20A}, N. Yu. Muchnoi^{9,d}, H. Muramatsu⁴⁷, A. Mustafa⁴, Y. Nefedov²⁴, F. Nefling¹⁰, I. B. Nikolaev^{9,d}, Z. Ning^{1,40}, S. S. Nisar⁸, S. L. Niu^{1,40}, X. Y. Niu^{1,44}, S. L. Olsen^{33,j}, Q. Ouyang^{1,40,44}, S. Pacetti^{20B}, Y. Pan^{50,40}, M. Papenbrock⁵⁴, P. Patteri^{20A}, M. Pelizzaeus⁴, J. Pellegrino^{53A,53C}, H. P. Peng^{50,40}, K. Peters^{10,g}, J. Pettersson⁵⁴, J. L. Ping²⁹, R. G. Ping^{1,44}, A. Pitka²³, R. Poling⁴⁷, V. Prasad^{50,40}, H. R. Qi², M. Qi³⁰, T. Y. Qi², S. Qian^{1,40}, C. F. Qiao⁴⁴, N. Qin⁵⁵, X. S. Qin⁴, Z. H. Qin^{1,40}, J. F. Qiu¹, K. H. Rashid^{52,i}, C. F. Redmer²³, M. Richter⁴, M. Ripka²³, M. Rolo^{53C}, G. Rong^{1,44}, Ch. Rosner¹⁴, X. D. Ruan¹², A. Sarantsev^{24,e}, M. Savri^{21B}, C. Schnier⁴, K. Schoenning⁵⁴, W. Shan³², M. Shao^{50,40}, C. P. Shen², P. X. Shen³¹, X. Y. Shen^{1,44}, H. Y. Sheng¹, J. J. Song³⁴, W. M. Song³⁴, X. Y. Song¹, S. Sosio^{53A,53C}, C. Sowa⁴, S. Spataro^{53A,53C}, G. X. Sun¹, J. F. Sun¹⁵, L. Sun⁵⁵, S. S. Sun^{1,44}, X. H. Sun¹, Y. J. Sun^{50,40}, Y. K. Sun^{50,40}, Y. Z. Sun¹, Z. J. Sun^{1,40}, Z. T. Sun¹⁹, C. J. Tang³⁷, G. Y. Tang¹, X. Tang¹, I. Tapan^{43C}, M. Tiemens²⁶, B. Tsednee²², I. Uman^{43D}, G. S. Varner⁴⁵, B. Wang¹, B. L. Wang⁴⁴, D. Wang³², D. Y. Wang³², Dan Wang⁴⁴, K. Wang^{1,40}, L. L. Wang¹, L. S. Wang¹, M. Wang³⁴, Meng Wang^{1,44}, P. Wang¹, P. L. Wang¹, W. P. Wang^{50,40}, X. F. Wang⁴², Y. Wang³⁸, Y. D. Wang¹⁴, Y. F. Wang^{1,40,44}, Y. Q. Wang²³, Z. Wang^{1,40}, Z. G. Wang^{1,40}, Z. H. Wang^{50,40}, Z. Y. Wang¹, Zongyuan Wang^{1,44}, T. Weber²³, D. H. Wei¹¹, P. Weidenkaff²³, S. P. Wen¹, U. Wiedner⁴, M. Wolke⁵⁴, L. H. Wu¹, L. J. Wu^{1,44}, Z. Wu^{1,40}, L. Xia^{50,40}, X. Xia³⁴, Y. Xia¹⁸, D. Xiao¹, H. Xiao⁵¹, Y. J. Xiao^{1,44}, Z. J. Xiao²⁹, Y. G. Xie^{1,40}, Y. H. Xie⁶, X. A. Xiong^{1,44}, Q. L. Xiu^{1,40}, G. F. Xu¹, J. J. Xu^{1,44}, L. Xu¹, Q. J. Xu¹³, Q. N. Xu⁴⁴, X. P. Xu³⁸, L. Yan^{53A,53C}, W. B. Yan^{50,40}, W. C. Yan², W. C. Yan^{50,40}, Y. H. Yan¹⁸, H. J. Yang^{35,h}, H. X. Yang¹, L. Yang⁵⁵, Y. H. Yang³⁰, Y. X. Yang¹¹, Yifan Yang^{1,44}, M. Ye^{1,40}, M. H. Ye⁷, J. H. Yin¹, Z. Y. You⁴¹, B. X. Yu^{1,40,44}, C. X. Yu³¹, J. S. Yu²⁷, C. Z. Yuan^{1,44}, Y. Yuan¹, A. Yuncu^{43B,a}, A. A. Zafar⁵², A. Zallo^{20A}, Y. Zeng¹⁸, Z. Zeng^{50,40}, B. X. Zhang¹, B. Y. Zhang^{1,40}, C. C. Zhang¹, D. H. Zhang¹, H. H. Zhang⁴¹, H. Y. Zhang^{1,40}, J. Zhang^{1,44}, J. L. Zhang¹, J. Q. Zhang¹, J. W. Zhang^{1,40,44}, J. Y. Zhang¹, J. Z. Zhang^{1,44}, K. Zhang^{1,44}, L. Zhang⁴², S. Q. Zhang³¹, X. Y. Zhang³⁴, Y. H. Zhang^{1,40}, Y. T. Zhang^{50,40}, Yang Zhang¹, Yao Zhang¹, Yu Zhang⁴⁴, Z. H. Zhang⁶, Z. P. Zhang⁵⁰, Z. Y. Zhang⁵⁵, G. Zhao¹, J. W. Zhao^{1,40}, J. Y. Zhao^{1,44}, J. Z. Zhao^{1,40}, Lei Zhao^{50,40}, Ling Zhao¹, M. G. Zhao³¹, Q. Zhao¹, S. J. Zhao⁵⁷, T. C. Zhao¹, Y. B. Zhao^{1,40}, Z. G. Zhao^{50,40}, A. Zhemchugov^{24,b}, B. Zheng⁵¹, J. P. Zheng^{1,40}, W. J. Zheng³⁴, Y. H. Zheng⁴⁴, B. Zhong²⁹, L. Zhou^{1,40}, X. Zhou⁵⁵, X. K. Zhou^{50,40}, X. R. Zhou^{50,40}, X. Y. Zhou¹, Y. X. Zhou¹², J. Zhu³¹, J. Zhu⁴¹, K. Zhu¹, K. J. Zhu^{1,40,44}, S. Zhu¹, S. H. Zhu⁴⁹, X. L. Zhu⁴², Y. C. Zhu^{50,40}, Y. S. Zhu^{1,44}, Z. A. Zhu^{1,44}, J. Zhuang^{1,40}, B. S. Zou¹, J. H. Zou¹

(BESIII Collaboration)

¹ Institute of High Energy Physics, Beijing 100049, People's Republic of China

² Beihang University, Beijing 100191, People's Republic of China

³ Beijing Institute of Petrochemical Technology, Beijing 102617, People's Republic of China

⁴ Bochum Ruhr-University, D-44780 Bochum, Germany

⁵ Carnegie Mellon University, Pittsburgh, Pennsylvania 15213, USA

⁶ Central China Normal University, Wuhan 430079, People's Republic of China

⁷ China Center of Advanced Science and Technology, Beijing 100190, People's Republic of China

- ⁸ COMSATS Institute of Information Technology, Lahore, Defence Road, Off Raiwind Road, 54000 Lahore, Pakistan
- ⁹ G.I. Budker Institute of Nuclear Physics SB RAS (BINP), Novosibirsk 630090, Russia
- ¹⁰ GSI Helmholtzcentre for Heavy Ion Research GmbH, D-64291 Darmstadt, Germany
- ¹¹ Guangxi Normal University, Guilin 541004, People's Republic of China
- ¹² Guangxi University, Nanning 530004, People's Republic of China
- ¹³ Hangzhou Normal University, Hangzhou 310036, People's Republic of China
- ¹⁴ Helmholtz Institute Mainz, Johann-Joachim-Becher-Weg 45, D-55099 Mainz, Germany
- ¹⁵ Henan Normal University, Xinxiang 453007, People's Republic of China
- ¹⁶ Henan University of Science and Technology, Luoyang 471003, People's Republic of China
- ¹⁷ Huangshan College, Huangshan 245000, People's Republic of China
- ¹⁸ Hunan University, Changsha 410082, People's Republic of China
- ¹⁹ Indiana University, Bloomington, Indiana 47405, USA
- ²⁰ (A)INFN Laboratori Nazionali di Frascati, I-00044, Frascati, Italy; (B)INFN and University of Perugia, I-06100, Perugia, Italy
- ²¹ (A)INFN Sezione di Ferrara, I-44122, Ferrara, Italy; (B)University of Ferrara, I-44122, Ferrara, Italy
- ²² Institute of Physics and Technology, Peace Ave. 54B, Ulaanbaatar 13330, Mongolia
- ²³ Johannes Gutenberg University of Mainz, Johann-Joachim-Becher-Weg 45, D-55099 Mainz, Germany
- ²⁴ Joint Institute for Nuclear Research, 141980 Dubna, Moscow region, Russia
- ²⁵ Justus-Liebig-Universitaet Giessen, II. Physikalisches Institut, Heinrich-Buff-Ring 16, D-35392 Giessen, Germany
- ²⁶ KVI-CART, University of Groningen, NL-9747 AA Groningen, The Netherlands
- ²⁷ Lanzhou University, Lanzhou 730000, People's Republic of China
- ²⁸ Liaoning University, Shenyang 110036, People's Republic of China
- ²⁹ Nanjing Normal University, Nanjing 210023, People's Republic of China
- ³⁰ Nanjing University, Nanjing 210093, People's Republic of China
- ³¹ Nankai University, Tianjin 300071, People's Republic of China
- ³² Peking University, Beijing 100871, People's Republic of China
- ³³ Seoul National University, Seoul, 151-747 Korea
- ³⁴ Shandong University, Jinan 250100, People's Republic of China
- ³⁵ Shanghai Jiao Tong University, Shanghai 200240, People's Republic of China
- ³⁶ Shanxi University, Taiyuan 030006, People's Republic of China
- ³⁷ Sichuan University, Chengdu 610064, People's Republic of China
- ³⁸ Soochow University, Suzhou 215006, People's Republic of China
- ³⁹ Southeast University, Nanjing 211100, People's Republic of China
- ⁴⁰ State Key Laboratory of Particle Detection and Electronics, Beijing 100049, Hefei 230026, People's Republic of China
- ⁴¹ Sun Yat-Sen University, Guangzhou 510275, People's Republic of China
- ⁴² Tsinghua University, Beijing 100084, People's Republic of China
- ⁴³ (A)Ankara University, 06100 Tandogan, Ankara, Turkey; (B)Istanbul Bilgi University, 34060 Eyup, Istanbul, Turkey; (C)Uludag University, 16059 Bursa, Turkey; (D)Near East University, Nicosia, North Cyprus, Mersin 10, Turkey
- ⁴⁴ University of Chinese Academy of Sciences, Beijing 100049, People's Republic of China
- ⁴⁵ University of Hawaii, Honolulu, Hawaii 96822, USA
- ⁴⁶ University of Jinan, Jinan 250022, People's Republic of China
- ⁴⁷ University of Minnesota, Minneapolis, Minnesota 55455, USA
- ⁴⁸ University of Muenster, Wilhelm-Klemm-Str. 9, 48149 Muenster, Germany
- ⁴⁹ University of Science and Technology Liaoning, Anshan 114051, People's Republic of China
- ⁵⁰ University of Science and Technology of China, Hefei 230026, People's Republic of China
- ⁵¹ University of South China, Hengyang 421001, People's Republic of China
- ⁵² University of the Punjab, Lahore-54590, Pakistan
- ⁵³ (A)University of Turin, I-10125, Turin, Italy; (B)University of Eastern Piedmont, I-15121, Alessandria, Italy; (C)INFN, I-10125, Turin, Italy
- ⁵⁴ Uppsala University, Box 516, SE-75120 Uppsala, Sweden
- ⁵⁵ Wuhan University, Wuhan 430072, People's Republic of China
- ⁵⁶ Zhejiang University, Hangzhou 310027, People's Republic of China
- ⁵⁷ Zhengzhou University, Zhengzhou 450001, People's Republic of China
- ^a Also at Bogazici University, 34342 Istanbul, Turkey
- ^b Also at the Moscow Institute of Physics and Technology, Moscow 141700, Russia
- ^c Also at the Functional Electronics Laboratory, Tomsk State University, Tomsk, 634050, Russia
- ^d Also at the Novosibirsk State University, Novosibirsk, 630090, Russia
- ^e Also at the NRC "Kurchatov Institute", PNPI, 188300, Gatchina, Russia
- ^f Also at Istanbul Arel University, 34295 Istanbul, Turkey
- ^g Also at Goethe University Frankfurt, 60323 Frankfurt am Main, Germany
- ^h Also at Key Laboratory for Particle Physics, Astrophysics and Cosmology, Ministry of Education; Shanghai Key Laboratory for Particle Physics and Cosmology; Institute of Nuclear and Particle Physics, Shanghai 200240, People's Republic of China
- ⁱ Government College Women University, Sialkot - 51310. Punjab, Pakistan.

^j Currently at: Center for Underground Physics, Institute for Basic Science, Daejeon 34126, Korea

Based on an e^+e^- collision data sample corresponding to an integrated luminosity of 567 pb^{-1} taken at the center-of-mass energy of $\sqrt{s} = 4.6 \text{ GeV}$ with the BESIII detector, we measure the absolute branching fraction of the inclusive decay $\Lambda_c^+ \rightarrow \Lambda + X$ to be $\mathcal{B}(\Lambda_c^+ \rightarrow \Lambda + X) = (38.2_{-2.2}^{+2.8} \pm 0.8)\%$ using the double-tag method, where X refers to any possible final state particles. In addition, we search for direct CP violation in the charge asymmetry of this inclusive decay for the first time, and obtain $\mathcal{A}_{CP} \equiv \frac{\mathcal{B}(\Lambda_c^+ \rightarrow \Lambda + X) - \mathcal{B}(\bar{\Lambda}_c^- \rightarrow \bar{\Lambda} + X)}{\mathcal{B}(\Lambda_c^+ \rightarrow \Lambda + X) + \mathcal{B}(\bar{\Lambda}_c^- \rightarrow \bar{\Lambda} + X)} = (2.1_{-6.6}^{+7.0} \pm 1.4)\%$, a statistically limited result with no evidence of CP violation.

PACS numbers: 14.20.Lq, 13.30.-a

The inclusive decay $\Lambda_c^+ \rightarrow \Lambda + X$, where X means any possible final state particles, is mediated by the $c \rightarrow s$ Cabibbo-favored (CF) transition that dominates the decays of the Λ_c^+ [1–3]. As the Λ_c^+ is the lightest charmed baryon, the decay rate of the $\Lambda_c^+ \rightarrow \Lambda + X$ is important to calibrate the amplitude of the CF transition in the charmed baryon sector in theory, which suffers from a large uncertainty in the non-perturbative QCD region [3]. For instance, the $\Lambda_c^+ \rightarrow \Lambda + X$ decay rate is an essential input in the calculation of the lifetimes of charmed baryons, whose current theoretical results largely deviate from the experimental measurements [3–5]. Furthermore, better understanding of the quark structure and decay dynamics in the $\Lambda_c^+ \rightarrow \Lambda + X$ benefits the research on heavier charmed baryons [6, 7]. Especially for those lesser-known charmed baryons with double- or triple-charm quarks, an improved and calibrated theoretical prediction on the $c \rightarrow s$ decay vertex is crucial for guiding experimental search [8, 9], such as the observation of the Ξ_{cc}^{++} at LHCb [10].

Measurements of the branching fraction (BF) of this decay were carried out only before 1992 by the SLAC Hybrid Facility Photon, Photon Emulsion and CLEO collaborations [11–13]. The average of their results gives $\mathcal{B}(\Lambda_c^+ \rightarrow \Lambda + X) = (35 \pm 11)\%$ [5], with an uncertainty larger than 30%. The three individual measurements show big discrepancies, and their average in the Particle Data Group (PDG) gives a poor fit quality of $\chi^2/\text{ndf} = 4.1/2$ and a low confidence level of 0.126 [5]. This is because they were not absolute measurements and substantial uncertainties could be underestimated. Hence, it is crucial to carry out an absolute measurement with improved precision. Furthermore, the sum of the BFs of the known exclusive decay final states involving the Λ in PDG is $(24.5 \pm 2.1)\%$ [5]. The difference between the inclusive and exclusive rates will point out the size of as yet unknown decays, which requires high precision measurement of $\mathcal{B}(\Lambda_c^+ \rightarrow \Lambda + X)$. In addition, precise knowledge of $\mathcal{B}(\Lambda_c^+ \rightarrow \Lambda + X)$ provides an essential input for exploring the decays of b -flavored hadrons involving a Λ_c^+ in the final states.

It has been confirmed that the Cabibbo-Kobayashi-Maskawa (CKM) mechanism embedded in the Standard Model (SM) is the main source of CP violation in the quark sector [14]. The impressive agreement on CP vi-

olation among the results from the s -quark and b -quark sectors [15, 16], calls for further checks in the less tested area of c -quark sector. The SM predictions for CP violation in the charm sector are tiny due to the hierarchical structure of the CKM matrix and the mass differences between the fermion generations. Any significant amount of CP violation would be an observation of physics beyond the SM, and therefore, the charmed baryon decays provide an opportunity to improve our knowledge on CP violation in and beyond the SM [17–20]. In this analysis, we search for direct CP violation by measuring the charge asymmetry of this inclusive decay $\mathcal{A}_{CP} \equiv \frac{\mathcal{B}(\Lambda_c^+ \rightarrow \Lambda + X) - \mathcal{B}(\bar{\Lambda}_c^- \rightarrow \bar{\Lambda} + X)}{\mathcal{B}(\Lambda_c^+ \rightarrow \Lambda + X) + \mathcal{B}(\bar{\Lambda}_c^- \rightarrow \bar{\Lambda} + X)}$.

The data used in this Letter comprise an integrated luminosity of 567 pb^{-1} [21], corresponding to about 1.0×10^5 $\Lambda_c^+ \bar{\Lambda}_c^-$ pairs [22]. The data set was collected with the BESIII detector at the center-of-mass energy $\sqrt{s} = 4.6 \text{ GeV}$. At this energy, the $\Lambda_c^+ \bar{\Lambda}_c^-$ pairs are produced near the production threshold with no additional hadrons, providing a clean environment for studying Λ_c^+ decays. By analyzing the data with the double-tag (DT) method [23], we perform the first measurement of the absolute BF for the inclusive decay $\Lambda_c^+ \rightarrow \Lambda + X$. Throughout this Letter, charge-conjugate modes are implicitly assumed, unless explicitly stated.

Details about the features and capabilities of the BESIII detector can be found in Ref. [24]. The response of the experimental apparatus is simulated with a GEANT4-based [25] Monte Carlo (MC) simulation package. The reactions in e^+e^- annihilations are generated by KKMC [26] and EVTGEN [27], with initial-state radiation (ISR) effects [28] and final-state radiation (FSR) effects [29] included. To study backgrounds, optimize event selection criteria and validate data analysis method, an inclusive MC sample is produced at $\sqrt{s} = 4.6 \text{ GeV}$. This sample consists of pair production of charmed mesons (D and D_s) and baryons (Λ_c^+), the ISR-produced ψ states and quantum electrodynamics processes. The Λ_c^+ is set to decay to all possible final states based on the BFs from the Particle Data Group (PDG) [30].

To study the signal $\Lambda_c^+ \rightarrow \Lambda + X$ with the DT method, we first select the anti-particle $\bar{\Lambda}_c^-$ by the two decay modes, $\bar{\Lambda}_c^- \rightarrow \bar{p}K_S^0$ and $\bar{\Lambda}_c^- \rightarrow \bar{p}K^+\pi^-$. The yield of

the tag mode i , N_i^{tag} , is given by

$$N_i^{\text{tag}} = 2 \cdot N_{\Lambda_c^+ \bar{\Lambda}_c^-} \cdot \mathcal{B}_i^{\text{tag}} \cdot \varepsilon_i^{\text{tag}}, \quad (1)$$

where $N_{\Lambda_c^+ \bar{\Lambda}_c^-}$ is the number of $\Lambda_c^+ \bar{\Lambda}_c^-$ pairs in the data sample, while $\mathcal{B}_i^{\text{tag}}$ and $\varepsilon_i^{\text{tag}}$ are the BF and detection efficiency for the tag mode i . Then we search for a Λ among the remaining tracks. The number of the inclusive decays of $\Lambda_c^+ \rightarrow \Lambda + X$ in the presence of the tag mode i , N_i^{sig} , is given by

$$N_i^{\text{sig}} = 2 \cdot N_{\Lambda_c^+ \bar{\Lambda}_c^-} \cdot \mathcal{B}_i^{\text{tag}} \cdot \mathcal{B}_i^{\text{sig}} \cdot \varepsilon_i^{\text{tag}} \cdot \varepsilon_i^{\text{sig}}, \quad (2)$$

where $\mathcal{B}_i^{\text{sig}}$ and $\varepsilon_i^{\text{sig}}$ are the BF and reconstruction efficiency for the inclusive decay $\Lambda_c^+ \rightarrow \Lambda + X$. Here we assume that the reconstruction efficiency $\varepsilon_i^{\text{sig}}$ is independent of the tag mode, so the DT efficiency is given by $\varepsilon_i^{\text{sig,tag}} \approx \varepsilon_i^{\text{sig}} \cdot \varepsilon_i^{\text{tag}}$. From Eq. (1) and Eq. (2) we determine the BF of the signal process by

$$\mathcal{B}_i^{\text{sig}} = \frac{(\sum_i N_i^{\text{sig}})/\varepsilon_i^{\text{sig}}}{\sum_i N_i^{\text{tag}}}. \quad (3)$$

The efficiency for detecting Λ as a function of momentum and polar angle is determined from data with a control sample of J/ψ decays. Due to lacking knowledge of the phase space distribution of the inclusive decay $\Lambda_c^+ \rightarrow \Lambda + X$, we re-weight the Λ efficiencies according to the momentum and polar angle distributions of Λ in the DT signals. Therefore, the signal BF is calculated by

$$\mathcal{B}_i^{\text{sig}} = \frac{\sum_j ((\sum_i N_{i,j}^{\text{sig}})/\varepsilon_j^{\text{sig}})}{\sum_i N_i^{\text{tag}}} = \frac{\sum_j (N_{-j}^{\text{sig}}/\varepsilon_j^{\text{sig}})}{\sum_i N_i^{\text{tag}}}, \quad (4)$$

where $j = 1, 2, \dots$ is the index for the intervals of Λ weighting kinematics, and N_{-j}^{sig} is the sum of DT signal yields in the two tag modes within the j -th interval.

To select the candidate events, the charged tracks detected in the main drift chamber (MDC) are required to satisfy $|\cos\theta| < 0.93$, where θ is the polar angle with respect to the direction of the e^+ beam. The distance of closest approach of the charged tracks to the run-averaged interaction point (IP) must be less than 10 cm along the beam axis and less than 1 cm in the perpendicular plane, except for those tracks used to reconstruct K_S^0 and Λ . Particle identification (PID) is achieved by combining the measurement of specific ionization (dE/dx) and time-of-flight information to compute likelihoods for different particle hypotheses. Protons are distinguished from pions and kaons with the likelihood requirements $\mathcal{L}(p) > \mathcal{L}(K)$ and $\mathcal{L}(p) > \mathcal{L}(\pi)$, while kaons and pions are discriminated from each other by requiring $\mathcal{L}(K) > \mathcal{L}(\pi)$ or $\mathcal{L}(\pi) > \mathcal{L}(K)$, respectively. To improve efficiency, no PID requirements are imposed on the charged pion candidates from the decays of Λ or K_S^0 .

The K_S^0 and Λ candidates are reconstructed through their dominant decays $K_S^0 \rightarrow \pi^+\pi^-$ and $\Lambda \rightarrow p\pi^-$. The distances of closest approach of the two candidate

TABLE I. Requirements on ΔE , M_{BC} and resulting yields N_i^{tag} for the tagged $\bar{\Lambda}_c^-$ in data. The uncertainty of N_i^{tag} is statistical only.

Tag mode i	ΔE (GeV)	M_{BC} (GeV/ c^2)	N_i^{tag}
$\bar{\Lambda}_c^- \rightarrow \bar{p}K_S^0$	[-0.021, 0.019]	[2.282, 2.300]	1220 ± 37
$\bar{\Lambda}_c^- \rightarrow \bar{p}K^+\pi^-$	[-0.020, 0.015]		6088 ± 85

charged tracks to the IP must be within ± 20 cm along the beam direction, with no requirements imposed in the perpendicular plane. The two charged tracks are constrained to originate from a common vertex by performing a vertex fit on the two tracks and requiring the χ^2 of the fit to be less than 100. A secondary vertex fit is performed on the daughter tracks of the surviving K_S^0 and Λ candidates, imposing the additional constraint that the momentum of the candidate points back to the IP. The decay vertex from this secondary vertex fit is required to be on the correct side of the IP and separated from the IP by a distance of at least twice its fitted resolution. The events with only one pair of charged tracks satisfying the above requirements are kept, and the fitted momenta of the $\pi^+\pi^-$ and $p\pi^-$ combinations are used in the further analysis. To select K_S^0 and Λ candidates, the invariant masses of $\pi^+\pi^-$ and $p\pi^-$ are required to be in the range $487 < M_{\pi^+\pi^-} < 511$ MeV/ c^2 and $1111 < M_{p\pi^-} < 1121$ MeV/ c^2 , respectively.

To distinguish the tagged $\bar{\Lambda}_c^-$ candidates from background, we define two variables in the e^+e^- rest frame that reflect the conservation of energy and momentum. The first is the energy difference, $\Delta E \equiv E_{\bar{\Lambda}_c^-} - E_{\text{beam}}$, where $E_{\bar{\Lambda}_c^-}$ is the measured energy of the tagged $\bar{\Lambda}_c^-$ candidate and E_{beam} is the beam energy. To suppress combinatorial backgrounds, the mode-dependent ΔE requirements listed in Table I, corresponding to ± 2.5 times the resolutions of the fitted ΔE peaks, are imposed on the tagged $\bar{\Lambda}_c^-$ candidates. The second is the beam-constrained mass of the tagged $\bar{\Lambda}_c^-$ candidate, $M_{\text{BC}} \equiv \sqrt{E_{\text{beam}}^2 - |\vec{p}_{\bar{\Lambda}_c^-}|^2 \cdot c^2/c^2}$, where $\vec{p}_{\bar{\Lambda}_c^-}$ represents the momentum of the $\bar{\Lambda}_c^-$ candidate. Figure 1 shows the M_{BC} distributions of the two tag modes, showing clear $\bar{\Lambda}_c^-$ signals at the expected mass. Studies based on MC show that the peaking backgrounds in the tag modes are negligible. Maximum likelihood fits are performed on these M_{BC} distributions to obtain the yields of tagged $\bar{\Lambda}_c^-$. The backgrounds are parameterized by an ARGUS function [31] with endpoint fixed to the beam energy. The signals are described by the MC-simulated shapes convoluted by Gaussian functions with free widths to account for the difference of resolutions between data and MC simulations. The yields for the background and signal are free parameters in the fits. By subtracting the number of events of the fitted backgrounds from the total event yields, we obtain the yields of the single tagged $\bar{\Lambda}_c^-$, as listed in Table I.

Then we search for a Λ candidate among the remaining

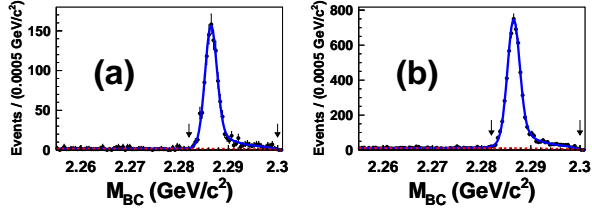


FIG. 1. Fits to the M_{BC} distributions of the candidate events for (a) $\bar{\Lambda}_c^- \rightarrow \bar{p}K_S^0$ and (b) $\bar{\Lambda}_c^- \rightarrow \bar{p}K^+\pi^-$ in data. The thick dots stand for the data. The solid curves denote the total fits, while the dotted lines represent the background. The arrows show the signal regions. The description of the fits is given in the text.

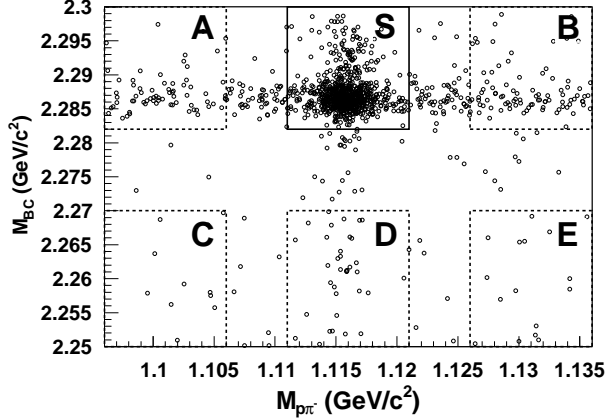


FIG. 2. Scatter plot of M_{BC} versus $M_{p\pi^-}$ of the DT candidates in data. The box labeled S stands for the signal region, while boxes A, B, C, D, and E denote the sideband regions.

tracks on the recoiling side of the tagged $\bar{\Lambda}_c^-$. The signal yield is determined from the distribution of M_{BC} versus the invariant mass of $p\pi^-$ system $M_{p\pi^-}$ by

$$N^{\text{sig}} = N^S - \frac{N^A + N^B}{2} - f \cdot (N^D - \frac{N^C + N^E}{2}), \quad (5)$$

where N^S , N^A , N^B , N^C , N^D and N^E represent the numbers of events observed in the regions of S, A, B, C, D and E, as shown in Fig. 2. Here the backgrounds due to misreconstruction of Λ are assumed to be flat in the $M_{p\pi^-}$ distribution, which can be estimated from the events in regions A and B. While the peaking backgrounds in the $M_{p\pi^-}$ distribution, which are from non- Λ_c^+ decays with Λ correctly reconstructed, can be estimated using the sideband region of M_{BC} , namely the regions C, D and E. f is the ratio of background area of the signal region over that of the sideband region in the M_{BC} distribution, which is evaluated to be 0.58 ± 0.06 from the fit to the combined M_{BC} distribution of data for the two tagging modes. We divide the data into 5×4 two-dimensional $(p, |\cos\theta|)$ intervals of Λ and obtain the net signal yield in each kinematic interval following Eq. (5), as listed in Table II.

TABLE II. Signal yield and detection efficiency of the inclusive Λ in each $(p, |\cos\theta|)$ interval. The uncertainties here are statistical only.

p (GeV/c)	N^{sig}			
	$ \cos\theta $			
	(0.00, 0.20)	(0.20, 0.40)	(0.40, 0.65)	(0.65, 1.00)
[0.0, 0.3]	$5.3^{+5.1}_{-3.8}$	$11.4^{+5.5}_{-4.2}$	$9.1^{+5.5}_{-4.2}$	$6.3^{+5.4}_{-4.0}$
[0.3, 0.5]	$59.8^{+9.9}_{-8.6}$	$41.6^{+8.9}_{-7.7}$	$71.9^{+10.7}_{-9.5}$	$33.1^{+8.7}_{-7.4}$
[0.5, 0.7]	$86.7^{+10.9}_{-9.7}$	$72.5^{+10.0}_{-8.8}$	$74.8^{+10.1}_{-9.0}$	$53.9^{+9.1}_{-7.9}$
[0.7, 0.9]	$40.4^{+7.8}_{-6.6}$	$28.3^{+6.8}_{-5.6}$	$44.0^{+8.1}_{-6.9}$	$38.4^{+7.9}_{-6.7}$
[0.9, 1.1]	$6.9^{+4.3}_{-3.0}$	$12.4^{+5.0}_{-3.7}$	$8.3^{+4.2}_{-2.9}$	$5.5^{+3.9}_{-2.6}$
p (GeV/c)	ϵ^{sig} (%)			
	$ \cos\theta $			
	(0.00, 0.20)	(0.20, 0.40)	(0.40, 0.65)	(0.65, 1.00)
[0.0, 0.3]	8.28 ± 0.38	8.22 ± 0.37	8.01 ± 0.31	4.45 ± 0.21
[0.3, 0.5]	29.03 ± 0.37	28.28 ± 0.37	26.56 ± 0.33	14.98 ± 0.21
[0.5, 0.7]	35.43 ± 0.32	35.00 ± 0.33	33.25 ± 0.32	20.15 ± 0.25
[0.7, 0.9]	39.68 ± 0.47	39.27 ± 0.50	36.56 ± 0.50	23.80 ± 0.51
[0.9, 1.1]	40.82 ± 0.14	40.21 ± 0.14	37.76 ± 0.12	29.97 ± 0.11

The efficiencies for detecting a Λ candidate are estimated from the control samples $J/\psi \rightarrow \Lambda\bar{\Lambda}$ and $J/\psi \rightarrow \bar{p}K^+\Lambda$, which are selected from a J/ψ on-peak data sample consisting of $(1310.6 \pm 7.0) \times 10^6$ J/ψ decays [32]. In each kinematic interval, the data-driven efficiency is calculated based on a ‘‘tag-and-probe’’ technique. For $J/\psi \rightarrow \Lambda\bar{\Lambda}$, a $\bar{\Lambda}$ is tagged in an event, while for $J/\psi \rightarrow \bar{p}K^+\Lambda$, two charged tracks identified as a proton and a kaon are selected. The missing Λ is identified by limiting the missing mass within $[1.067, 1.155]$ GeV/c^2 for $J/\psi \rightarrow \Lambda\bar{\Lambda}$ and $[1.093, 1.139]$ GeV/c^2 for $J/\psi \rightarrow \bar{p}K^+\Lambda$. In the tagged event, we search for a Λ among the remaining tracks and take the detection rate as the efficiency. We partition the control samples into $(p, |\cos\theta|)$ intervals, and then determine the efficiency in each interval, as listed in Table II. For these efficiencies, the BF of the intermediate process $\Lambda \rightarrow p\pi^-$ has been included, and the uncertainties are statistical only. Inserting the numbers of N_i^{tag} from Table I, and the numbers of N_{-j}^{sig} and ϵ_j^{sig} from Table II into Eq. (4), we determine the BF of $\Lambda_c^+ \rightarrow \Lambda + X$ to be $\mathcal{B}(\Lambda_c^+ \rightarrow \Lambda + X) = (38.2^{+2.8}_{-2.3})\%$. The reliability of the analysis method used in this work has been validated by analyzing the inclusive MC sample.

The CP asymmetry of the decay $\Lambda_c^+ \rightarrow \Lambda + X$ is obtained by comparing the separate BFs of the charge conjugate decays, which are $\mathcal{B}(\Lambda_c^+ \rightarrow \Lambda + X) = (39.4^{+4.7}_{-3.4})\%$ and $\mathcal{B}(\bar{\Lambda}_c^- \rightarrow \bar{\Lambda} + X) = (37.8^{+3.8}_{-2.9})\%$. The yields and efficiencies of $\Lambda_c^+ \rightarrow \Lambda + X$ and $\bar{\Lambda}_c^- \rightarrow \bar{\Lambda} + X$ can be found in the supplemental material [33]. The CP asymmetry is determined to be $\mathcal{A}_{CP} = (2.1^{+7.0}_{-6.6})\%$, where the uncertainty is statistical only.

In the BF measurement with the DT method, systematic uncertainties from the tag side mostly cancel. Other non-canceling systematic uncertainties, which are estimated relative to the measured BF, are discussed below. The limited statistics of the Λ control samples bring uncertainty to the Λ efficiency, which is estimated by a weighted root-mean-square (RMS) of the statisti-

cal uncertainties for different $(p, |\cos\theta|)$ intervals given in Table II. In this analysis, the efficiency for reconstructing a $\bar{\Lambda}_c^-$ using the tag modes or finding a Λ in the Λ_c^+ side have been assumed to be independent of the multiplicities of the $\Lambda_c^+/\bar{\Lambda}_c^-$ sides. To evaluate the potential bias of this assumption, we use MC simulation to study the Λ efficiencies with 2 different tag modes, or the tag efficiencies with and without inclusion of non- Λ -involved Λ_c^+ decays in the signal side. We find the resultant changes on the Λ efficiency or tag efficiency are at the percent level, which are taken as the systematic uncertainties. The choice of kinematic intervals is varied and the resultant changes on the output BF are examined. The maximum change is quoted as the systematic uncertainty. The uncertainty due to the fitting procedure of tag yields is studied by altering the signal shape, fitting range and endpoint of the ARGUS function. Potential bias of the background-subtraction procedure in Eq. (5) is studied by changing the boundaries of sideband regions and taking the largest difference in the resultant BF as the systematic uncertainty. All of the above systematic uncertainties are summarized in Table III and the total uncertainty is determined to be 2.3% as the sum in quadrature. For the charge asymmetry \mathcal{A}_{CP} , we assume that the systematic uncertainties for the channels of Λ and $\bar{\Lambda}$ are the same and completely uncorrelated.

TABLE III. Summary of the relative systematic uncertainties for the BF of $\Lambda_c^+ \rightarrow \Lambda + X$.

Source	Relative uncertainty (%)
Statistics of the control sample	0.6
Λ efficiency bias	1.1
Tag efficiencies bias	1.6
Choices of the intervals	0.5
Tag yields	0.9
Background subtraction	0.3
Total	2.3

In summary, by analyzing a data sample taken at $\sqrt{s} = 4.6$ GeV with the BESIII detector, we report the absolute BF of the inclusive decay of $\Lambda_c^+ \rightarrow \Lambda + X$ to be

$\mathcal{B}(\Lambda_c^+ \rightarrow \Lambda + X) = (38.2_{-2.2}^{+2.8} \pm 0.8)\%$. The precision of the BF is improved by a factor of 4 compared to previous measurements [5]. This inclusive rate is larger than the exclusive rate of $(24.5 \pm 2.1)\%$ in PDG [5], which indicates that more than one third of the Λ_c^+ decays to Λ remain unobserved in experiment. Furthermore, we search for direct CP violation in this decay for the first time. The CP asymmetry is measured to be $\mathcal{A}_{CP} = (2.1_{-6.6}^{+7.0} \pm 1.4)\%$. The precision is limited by statistical uncertainty and no evidence for CP violation is found.

The authors would like to thank Hai-Yang Cheng and Fu-Sheng Yu for useful discussions. The BESIII collaboration thanks the staff of BEPCII and the IHEP computing center for their strong support. This work is supported in part by National Key Basic Research Program of China under Contract No. 2015CB856700; National Natural Science Foundation of China (NSFC) under Contracts Nos. 11335008, 11425524, 11625523, 11635010, 11735014; the Chinese Academy of Sciences (CAS) Large-Scale Scientific Facility Program; the CAS Center for Excellence in Particle Physics (CCEPP); Joint Large-Scale Scientific Facility Funds of the NSFC and CAS under Contracts Nos. U1532257, U1532258, U1732263; CAS Key Research Program of Frontier Sciences under Contracts Nos. QYZDJ-SSW-SLH003, QYZDJ-SSW-SLH040; 100 Talents Program of CAS; INPAC and Shanghai Key Laboratory for Particle Physics and Cosmology; German Research Foundation DFG under Contracts Nos. Collaborative Research Center CRC 1044, FOR 2359; Istituto Nazionale di Fisica Nucleare, Italy; Koninklijke Nederlandse Akademie van Wetenschappen (KNAW) under Contract No. 530-4CDP03; Ministry of Development of Turkey under Contract No. DPT2006K-120470; National Science and Technology fund; The Swedish Research Council; U. S. Department of Energy under Contracts Nos. DE-FG02-05ER41374, DE-SC-0010118, DE-SC-0010504, DE-SC-0012069; University of Groningen (RuG) and the Helmholtzzentrum fuer Schwerionenforschung GmbH (GSI), Darmstadt.

-
- | | |
|---|---|
| <p>[1] J. G. Körner, G. Kramer and J. Willrodt, Phys. Lett. B 78, 492 (1978) Erratum: [Phys. Lett. B 81, 419 (1979)].</p> <p>[2] D. M. Asner <i>et al.</i>, Int. J. Mod. Phys. A 24, S1 (2009).</p> <p>[3] H. Y. Cheng, Front. Phys. (Beijing) 10, 101406 (2015).</p> <p>[4] H. Y. Cheng, Phys. Rev. D 56, 2783 (1997).</p> <p>[5] C. Patrignani <i>et al.</i> (Particle Data Group), Chin. Phys. C 40, 100001 (2016) and 2017 update.</p> <p>[6] H. Y. Cheng and B. Tseng, Phys. Rev. D 46, 1042 (1992) Erratum: [Phys. Rev. D 55, 1697 (1997)].</p> <p>[7] H. Y. Cheng and B. Tseng, Phys. Rev. D 48, 4188 (1993).</p> <p>[8] C. Q. Geng, Y. K. Hsiao, C. W. Liu and T. H. Tsai, arXiv:1709.00808 [hep-ph].</p> <p>[9] F. S. Yu, H. Y. Jiang, R. H. Li, C. D. Lü, W. Wang and Z. X. Zhao, arXiv:1703.09086 [hep-ph].</p> | <p>[10] R. Aaij <i>et al.</i> (LHCb Collaboration), Phys. Rev. Lett. 119, 112001 (2017).</p> <p>[11] K. Abe <i>et al.</i> (SLAC Hybrid Facility Photon Collaboration), Phys. Rev. D 33, 1 (1986).</p> <p>[12] M. Adamovich <i>et al.</i> (Photon Emulsion Collaboration), Europhys. Lett. 4, 887 (1987).</p> <p>[13] G. D. Crawford <i>et al.</i> (CLEO Collaboration), Phys. Rev. D 45, 752 (1992).</p> <p>[14] M. Kobayashi and T. Maskawa, Prog. Theor. Phys. 49, 652 (1973).</p> <p>[15] J. Charles <i>et al.</i> (CKMfitter Group), Eur. Phys. J. C 41 (2005) no.1, 1. Updates at ckmfitter.in2p3.fr.</p> <p>[16] M. Bona <i>et al.</i> (UTfit Collaboration), JHEP 0507, 028 (2005). Updates at www.utfit.org</p> |
|---|---|

- [17] J. Charles, S. Descotes-Genon, X. W. Kang, H. B. Li and G. R. Lu, Phys. Rev. D **81**, 054032 (2010).
- [18] X. W. Kang and H. B. Li, Phys. Lett. B **684**, 137 (2010).
- [19] X. W. Kang, H. B. Li, G. R. Lu and A. Datta, Int. J. Mod. Phys. A **26**, 2523 (2011).
- [20] M. Bobrowski, A. Lenz, J. Riedl and J. Rohrwild, JHEP **1003**, 009 (2010).
- [21] M. Ablikim *et al.* (BESIII Collaboration), Chin. Phys. C **39**, 093001 (2015).
- [22] M. Ablikim *et al.* (BESIII Collaboration), Phys. Rev. Lett. **116**, 052001 (2016).
- [23] R. M. Baltrusaitis *et al.* (MARK-III Collaboration), Phys. Rev. Lett. **56**, 2140 (1986).
- [24] M. Ablikim *et al.* (BESIII Collaboration), Nucl. Instrum. Meth. A **614**, 345 (2010).
- [25] S. Agostinelli *et al.* (GEANT4 Collaboration), Nucl. Instrum. Meth. A **506**, 250 (2003).
- [26] S. Jadach, B. F. L. Ward and Z. Was, Comput. Phys. Commun. **130**, 260 (2000); Phys. Rev. D **63**, 113009 (2001).
- [27] D. J. Lange, Nucl. Instrum. Meth. A **462**, 152 (2001); R. G. Ping, Chin. Phys. C **32**, 599 (2008).
- [28] E. A. Kuraev and V. S. Fadin, Sov. J. Nucl. Phys. **41**, 466 (1985) [Yad. Fiz. **41**, 733 (1985)].
- [29] E. Richter-Was, Phys. Lett. B **303**, 163 (1993).
- [30] K. A. Olive *et al.* (Particle Data Group), Chin. Phys. C **40**, 100001 (2014).
- [31] H. Albrecht *et al.* (ARGUS Collaboration), Phys. Lett. B **241**, 278 (1990).
- [32] M. Ablikim *et al.* (BESIII Collaboration), Chin. Phys. C **41**, 013001 (2017).
- [33] See Supplemental Materials at [URL will be inserted by the publisher] for a summary of the yields of $\Lambda_c^+ \rightarrow \Lambda + X$ and $\bar{\Lambda}_c^- \rightarrow \bar{\Lambda} + X$, as well as the reconstruction efficiencies of Λ and $\bar{\Lambda}$.

SUPPLEMENTAL MATERIAL

TABLE IV. Signal yields and detection efficiencies of the inclusive Λ and $\bar{\Lambda}$ in each $(p, |\cos\theta|)$ interval. The errors here reflect only statistical uncertainties.

p (GeV/ c)	$N_{-,j}^{\text{sig},\Lambda}$				$N_{-,j}^{\text{sig},\bar{\Lambda}}$			
	$ \cos\theta $				$ \cos\theta $			
	[0.00, 0.20)	[0.20, 0.40)	[0.40, 0.65)	[0.65, 1.00)	[0.00, 0.20)	[0.20, 0.40)	[0.40, 0.65)	[0.65, 1.00)
[0.0, 0.3)	$4.5^{+3.7}_{-2.4}$	$4.2^{+4.3}_{-3.0}$	$5.9^{+4.4}_{-3.1}$	$6.8^{+4.6}_{-3.3}$	$0.8^{+4.4}_{-3.0}$	$7.2^{+4.3}_{-3.0}$	$3.2^{+4.3}_{-2.9}$	$-0.5^{+3.8}_{-2.4}$
[0.3, 0.5)	$26.8^{+7.2}_{-5.9}$	$17.8^{+6.2}_{-5.0}$	$44.7^{+8.3}_{-7.1}$	$11.5^{+6.0}_{-4.7}$	$33.0^{+7.6}_{-6.4}$	$23.8^{+7.2}_{-5.9}$	$27.2^{+7.5}_{-6.3}$	$21.6^{+7.1}_{-5.8}$
[0.5, 0.7)	$46.8^{+8.3}_{-7.2}$	$35.0^{+7.1}_{-5.9}$	$30.8^{+7.1}_{-5.9}$	$30.8^{+7.1}_{-5.9}$	$39.8^{+7.8}_{-6.6}$	$37.5^{+7.8}_{-6.6}$	$44.0^{+8.0}_{-6.8}$	$23.1^{+6.6}_{-5.3}$
[0.7, 0.9)	$21.5^{+6.0}_{-4.8}$	$14.4^{+5.2}_{-4.0}$	$21.0^{+6.0}_{-4.8}$	$17.9^{+5.9}_{-4.7}$	$18.9^{+5.9}_{-4.6}$	$13.9^{+5.3}_{-4.1}$	$23.0^{+6.2}_{-5.0}$	$20.5^{+6.0}_{-4.8}$
[0.9, 1.1)	$3.0^{+3.2}_{-1.8}$	$7.0^{+3.9}_{-2.7}$	$4.0^{+3.4}_{-2.1}$	$4.5^{+3.7}_{-2.4}$	$3.9^{+3.8}_{-2.5}$	$5.4^{+4.0}_{-2.6}$	$4.3^{+3.4}_{-2.2}$	$1.0^{+2.6}_{-1.2}$
p (GeV/ c)	$\varepsilon_j^{\text{sig},\Lambda}$ (%)				$\varepsilon_j^{\text{sig},\bar{\Lambda}}$ (%)			
	$ \cos\theta $				$ \cos\theta $			
	[0.00, 0.20)	[0.20, 0.40)	[0.40, 0.65)	[0.65, 1.00)	[0.00, 0.20)	[0.20, 0.40)	[0.40, 0.65)	[0.65, 1.00)
[0.0, 0.3)	7.98 ± 0.53	8.25 ± 0.52	7.75 ± 0.44	3.85 ± 0.27	8.54 ± 0.53	8.18 ± 0.52	8.24 ± 0.45	4.99 ± 0.30
[0.3, 0.5)	30.38 ± 0.55	29.38 ± 0.55	27.01 ± 0.48	15.53 ± 0.32	27.83 ± 0.50	27.30 ± 0.50	26.16 ± 0.45	14.49 ± 0.29
[0.5, 0.7)	35.92 ± 0.47	35.91 ± 0.49	34.14 ± 0.47	20.49 ± 0.36	35.02 ± 0.43	34.22 ± 0.44	32.49 ± 0.43	19.85 ± 0.34
[0.7, 0.9)	40.15 ± 0.70	39.30 ± 0.72	36.51 ± 0.71	24.05 ± 0.75	39.30 ± 0.64	39.26 ± 0.68	36.60 ± 0.69	23.56 ± 0.71
[0.9, 1.1)	41.34 ± 0.20	40.70 ± 0.19	38.38 ± 0.17	30.72 ± 0.16	40.30 ± 0.19	39.74 ± 0.16	37.17 ± 0.16	29.25 ± 0.15